

## Size effects in the electronic properties of hydrogen and helium embedded in small metal clusters: The self-consistent spherical-jellium-particle model

W. Ekardt

*Fritz-Haber-Institut der Max-Planck-Gesellschaft, Faradayweg 4-6, D-1000 Berlin 33, West Germany*

(Received 4 June 1987)

The electronic properties of H and He, as the simplest examples for reactive and inert atomic systems embedded in small metal clusters, are investigated within the self-consistent spherical-jellium-particle model. Physical properties of interest are the modification of the electronic properties of the jellium particle (as a model for real clusters of the *sp*-bonded metals) by light impurities and vice versa, the modification of the free-atom properties when the atom is embedded in a metallic host which exhibits size-dependent quantum-mechanical properties. Quantities investigated include size-dependent impurity ionization potentials, relaxation shifts and static screening properties, size-dependent impurity immersion energies, and size-dependent impurity-induced quenching of the collective modes in small metal particles. Among other predictions it is demonstrated how the so-called magic numbers are modified by impurity embedding. The experimental verification of these predictions could give additional evidence for the electronic shell model for these particles.

### I. INTRODUCTION

There is ample evidence now that the jellium model for the description of the electronic properties of the clusters of the *sp*-bonded metals<sup>1-6</sup> such as Li, Na, K, Cu, Ag, and Au gives an excellent first-order prediction of the trends in the size dependence of the various experimentally observed data. Physical properties investigated so far include the so-called magic numbers in the abundance spectra,<sup>6-11</sup> the static polarizability,<sup>12</sup> and the ionization potentials and efficiencies<sup>13</sup> as a function of size. All these properties show characteristic discontinuities whenever a spherical shell is being completely filled. (For discontinuities related to spheroidal subshells, see Ref. 14.)

On the other hand, there is a long tradition of using the jellium model in studying the electronic properties of impurities in metals where generally, the impurity can be an interstitial or a substitutional one.<sup>15-23</sup> The extension of these kinds of studies to the jellium-cluster work seems to be of some relevance because problems like the size dependence of the Mahan-Nozières-de Dominicis edge-singularity problem<sup>24,25</sup> (and the related problem of size-dependent core-level shifts) are easiest to study within a simple but realistic model. So the philosophy is to describe the impurity atoms at a strictly microscopic level and for the description of the metallic host to use once more the model of a jellium cluster.

To the best of my knowledge, there is only one published study<sup>4</sup> of the size dependence of H embedded in a spherical jellium particle. Whereas the authors of Ref. 4 were mainly interested in the convergence of some static properties towards their bulk values (e.g., the electronic contact density at the impurity and its relevance for the Knight shift), the main interest in the present study is the size dependence of the spectroscopic properties of the coupled impurity-cluster system. So we hope that the

present study and the work of Hintermann and Manninen<sup>4</sup> complement each other in learning something about the properties of impurities in small metal particles. In addition, the present study aims at working out the characteristic differences between an inert system like He and a reactive one like H. As we shall see, the inert one is not as inert as some experimentalists would like to have it when performing matrix-isolation studies on, e.g., Ag embedded in Ar.

The rest of the paper is organized as follows: Sec. II gives a discussion of the static properties of the neutral particle and the ionized one. Sec. III turns to the discussion of the dynamical properties, and Sec. IV contains the conclusions.

### II. STATIC PROPERTIES

#### A. The method and the model

The method of calculation is—as in our previous work<sup>2</sup>—the local density approximation (LDA) with the exchange-correlation part of the functional approximated as proposed by Gunnarsson and Lundqvist.<sup>26</sup> The impurity, H or He, is placed at the center of the sphere to preserve the spherical symmetry of the resulting Kohn-Sham equations. Effects of moving the impurity around are discussed at the end. The ionic charge of the cluster is homogeneously smeared out to give a rigid, positively charged background of a certain  $r_s$  value, corresponding to a given ionic charge density. The motivation as well as a possible justification for this procedure were discussed in Ref. 2, and were afterwards experimentally confirmed by Knight *et al.*<sup>6</sup> and by Katakuse *et al.*<sup>9</sup> Furthermore, as shown by Geguzin,<sup>27</sup> by Cleland and Cohen,<sup>28</sup> by Rao *et al.*,<sup>29</sup> by Martins, Buttet, and Car,<sup>30</sup> and by Redfern, Chaney, and Rudolf.<sup>31</sup> The originally made assumption about the weakness of the ionic potentials due to their

pseudoion character is fulfilled to a high degree and, as a consequence, the electronic structure of the loosely bound valence electrons indeed resembles that of a liquid droplet, an object which could be called the "Sommerfeld droplet."<sup>32</sup>

The remaining deformation of the droplet by open-shell effects is presently under study in a strictly self-consistent fashion<sup>33</sup> with first results coming out very soon. From the first preliminary results it can be seen that the Nilsson model applied by Clemenger<sup>14</sup> is too crude an approximation to the self-consistent single-particle potential of a deformable jellium cluster.

The resulting Kohn-Sham equations which must be solved self-consistently agree with those of the pure jellium cluster, discussed in detail in Ref. 2. The only additional feature is a positive delta-function potential of strength +1 for H and of strength +2 for He. As a result, the numerics are slightly more demanding, but not too difficult. The total-energy functional remains the same, except for an additional term describing the electrostatic interaction with the impurity nuclear potential.

Because the behavior of H and He is rather different, the ground-state properties of these two impurities are discussed separately.

## B. Results

### 1. Hydrogen

As remarked above, the ground-state properties of H embedded in an infinite jellium were studied in the 1970's in a number of papers by Zaremba *et al.*, by Manninen and co-workers, by Jena and Singwi, and by others.<sup>15-23</sup> From these studies we know that, due to a bound state

just below the bottom of the single-particle potential at all metallic densities investigated, the electronic structure resembles that of a negative ion. Hence, one of the interesting questions to answer is, what is happening to this bound state as the size of the jellium cluster is reduced, because at small sizes metallic screening starts losing its meaning and, as a result, the H recovers its identity and finds itself as a negative ion (for  $r_s \rightarrow \infty$ ). The  $r_s$  value used in the calculation is 5.448,<sup>34</sup> and the numbers of electrons studied are  $N = 138, 58, 20$ , and 8. We believe that one  $r_s$  value and these few numbers, covering a diameter from, roughly, 30 Å down to 10 Å is just enough to see what is going on. From our earlier studies and from the work done by other authors we know how the results scale with the  $r_s$  value. So we really don't need a proliferation of theoretical data to make the principles clear.

In order to see more clearly the influence of the impurity we give at the beginning of the discussion the bare jellium-cluster results for each electron number. Hence, Fig. 1, left panel, shows the self-consistent electronic charge density, single-particle potential, and the single-particle levels occupied in the ground state for  $N = 138$ , which consist of 13 completely filled shells in the following order: 1s, 1p, 1d, 2s, 1f, 2p, 1g, 2d, 1h, 3s, 1i, 2f, 3p, with 3p being the top level.

This figure is similar to those published before for  $r_s = 4$  in Ref. 2 and for coated particles in Ref. 35. Hence, the interested reader who is not familiar with these figures and with the quantum numbers used is referred to the published work of the present author and to the work of others.

The situation changes significantly upon H embedding.

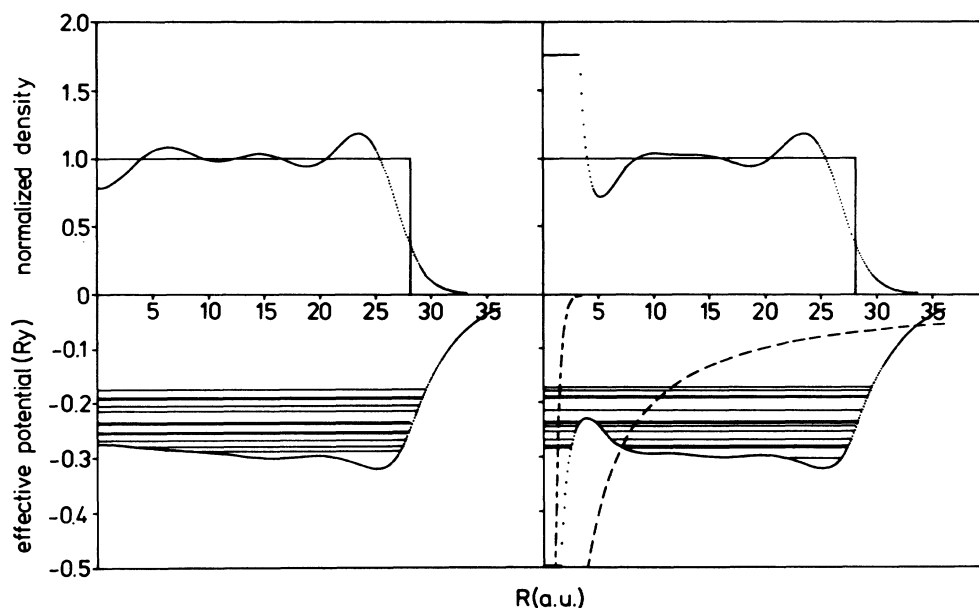


FIG. 1. Self-consistent charge density and single-particle potential of a jellium cluster with  $N = 138$  electrons and a background density parameter  $r_s = 5.448$  without (left panel) and with (right panel) H embedded. The charge density is in units of  $u_0 = 1/(4\pi/3)r_s^3$ , the potential is in Ry, and the length scale is in Bohr radii. The occupied single-particle levels in the ground state are given as straight lines. The potential hump around the H atom (an indication for overscreening) is already known from the infinite bulk system. In the impurity case, the bare proton potential (dashed line) and the total electrostatic potential of the hydrogen atom in vacuum (dash-dotted line) are given for comparison.

The right panel of Fig. 1 shows charge density and potential where, in addition, the bare proton potential and the neutral hydrogen potential in vacuum are shown for comparison. The overscreening of the potential, which can clearly be seen is known from the infinite jellium behavior and is an indication for the  $H^-$  state of the embedded hydrogen. The formerly empty  $4s$  level is pulled down below the  $3p$  level and now accommodates two electrons, whereas the topmost  $3p$  level is incompletely filled with just 5 electrons. The lowest level is rather different from the bare hydrogenic state, because it is extremely shallow and because of its charge localization both around the center of the particle and at the surface, where the latter effect is due to the typical potential fluctuations discussed in our previous work.<sup>2</sup>

Despite the quantization of the single-particle levels, the quantitative results are very similar to those of infinite jellium. This can most clearly be seen by comparing the Friedel oscillations of the total screening charge (shown in Fig. 2) with the corresponding results for infinite jellium, Refs. 18–21. Even the contact density at the proton deviates only by a few percent and the immersion energy, compiled in Table I, is similar to that of the infinite jellium system at this density, known to be equal to  $-1.62$  eV (from Refs. 18 or 23). Here, we have defined the immersion energy as

$$\Delta E = E_{\text{total}}(N, r_s; H) - E_{\text{total}}(N, r_s) - E_{\text{total}}(H),$$

with the total energy of H given by  $-13.381$  eV (calculated in the local spin-density approximation<sup>23</sup>). Looking at the figures, this near agreement with the infinite jellium values is quite understandable because the embedded

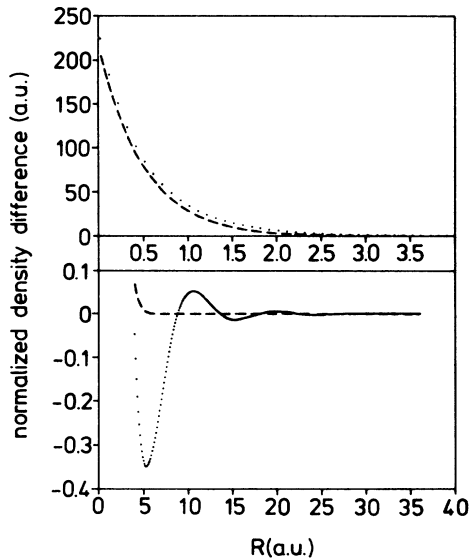


FIG. 2. Charge density difference around the proton in the system of Fig. 1. The charge density difference is (again) in units of  $n_0$  and the  $1s$  electron density of the H atom in vacuum is shown as dashed line. The Friedel oscillations are clearly resolved. Except for these oscillations the “size” of H is, in the embedded state, nearly the same as that of H in vacuum. The formation of the negative ion is clearly seen from the upper part of the figure.

TABLE I. Immersion energies  $\Delta E$  (in eV) for the embedding of H and He as a function of size  $R$  and electron number  $N$ . The  $r_s$  value is 5.448. The radius  $R$  of the particle is in Bohr radii. The energies are given with respect to the free-atom values of the LSDA (H)  $-13.381$  eV and the LDA (He)  $-77.852$  eV.

$N$	$R$	H	He
138	28.154	$-1.493$	0.339
58	21.089	$-1.528$	0.345
20	14.788	$-1.973$	0.691
8	10.986	$-1.973$	0.275

H is fairly localized.

Due to the potential fluctuations there is no clear-cut way for the determination of the energy of the bound state with respect to the bottom of the potential. However, one reasonable way could be the following: In the infinite system the energy of the lowest band state agrees, of course, with the bottom of the potential. Hence, a meaningful number for the energy of the bound state with respect to the band states would be given by the energy difference between the ground level and its neighbor. These values are compiled in Table II. The number for  $N = 138$  is indeed very similar to the value known for the infinite system.<sup>36</sup>

Next, we turn to the discussion of the ionization potential. There are at least three interesting points related with the presence of the impurity.

- (1) How does the ionization potential of the jellium cluster change upon impurity embedding?
- (2) How does the impurity ionization potential change upon its immersion?
- (3) How are these numbers related to the single-particle eigenvalues?

Here, the ionization potential of the cluster is defined, as usual, as the energy difference between the total energy of the system in the singly ionized state and the total energy of the neutral system, both calculated in their respective ground states. For the calculation of the impurity ionization potential upon immersion we perform a so-called  $\Delta$ SCF calculation. That means the total energy of the system is calculated with one electron missing in a shell other than the top-level shell. The procedure for calculating the self-consistent charge density and total energy of this (highly excited) state is exactly the same as for the ground state<sup>37</sup> and normally converges towards a stable result.<sup>37</sup> If so, the ionization potential of the impurity

TABLE II. Bound-state binding energies (in Ry) with respect to the lowest band state. In all cases the symmetry of the bound state is  $1s$  and that of the lowest band state is  $2s$ .

$N$	$R$	H	He
138	28.154	0.0178	0.930
58	21.089	0.0393	0.952
20	14.788	0.0764	0.943
8	10.986		0.957

purity upon immersion is just the energy difference between this fully relaxed (but highly excited) state with one impurity electron missing and the energy of the ground state. Here, we identify the impurity electron as one of the two electrons residing in the  $1s$  shell, because it is this shell which is split off the bottom of the potential.

In the following we designate the different ionization potentials by the symbol  $I$  with a subscript index referring to the electronic shell from which the electron is kicked off. Hence, the cluster ionization potential is  $I_{3p}$  and the impurity ionization potential is  $I_{1s}$ .

The answers to all the questions above are compiled in Table III. First of all, the change in the cluster ionization potential is small. This is to be expected, because  $N$  is already a very large number, and the impurity screening is a localized process. On the other hand, for the embedded H, the top-most impurity bound state (the only one for a system like H) loses its identity nearly completely. Hence, the huge change in the ionization potential from 13.381 eV for H in vacuum [calculated within the local-spin-density approximation<sup>23</sup> (LSDA)] to the value of 4.530 eV is quite understandable. It is just another way of saying that H is more or less incorporated into the cluster. This means the free bound state is nearly transformed to a band state. Therefore, the energy difference in these two different ways of cluster ionization nearly agrees with the difference in the corresponding single-particle levels because the self energy of a hole in the extended metallic band does not vary dramatically with its quantum number.<sup>38</sup> As we shall see below, the situation is completely different for He, because He preserves its identity at all metallic densities, which means that at all metallic densities the He core sustains one bound state well-separated from the bottom of the potential.

Having discussed in detail the behavior for  $N = 138$ , we turn now to the discussion of the other electron numbers, namely  $N = 58$ , 20, and 8. The results for  $N = 58$  are very similar to those for  $N = 138$ .

The symmetry of the single-particle levels without H is, in this order,  $1s, 1p, 1d, 2s, 1f, 2p, 1g$ , whereas in the presence of H there is some level rearrangement, namely  $1s, 2s, 1p, 1d, 1f, 3s, 2p, 1g$ . As before, the energies of the levels other than the  $s$  levels are nearly unchanged whereas the  $s$  levels, of course, are strongly influenced. As discussed below, this has some consequences for the magic numbers. The immersion energy of  $-1.528$  eV (see Table I) and the various ionization potentials (see

Table II) show only a weak size dependence, just as if we were discussing an extended physical system. Only the difference between the  $1s$  "bound state" and the state  $2s$  changes appreciably (not on an absolute scale) which is understandable because of the fluctuation of the bottom of the potential itself. Generally, one could say that H embedded in a particle of this size still behaves very much as if it were embedded in an infinite system.

The situation starts changing dramatically for  $N = 28$ , shown in Fig. 3. The level scheme with and without H, respectively, is  $1s, 1p, 1d, 2s$  and  $1s, 2s, 1p, 1d, 1f$ , where the  $1f$  shell contains just one electron. The immersion energy of  $-1.973$  eV shows the strong fluctuation known from Hintermanns work for Li (Ref. 4) and is related to the (size-induced) strong charge density fluctuations at the place where the H is residing. If one has in mind that H embedding is a fairly localized process, and if one remembers the density dependence of the immersion energy of H in an infinite jellium (Refs. 19 and 23) one immediately concludes that H diffusion would lead to H enrichment at the center of the sphere. This is so because the immersion energy as a function of the density has an absolute minimum at  $n = 0.0026$  a.u. and  $r = 5.4481$  corresponds to  $n = 0.00148$  a.u. It remains to be verified whether or not this would really take place. Whereas the ionization from the top level is still very similar with and without H, the "impurity" ionization potential is now dramatically changing. The value of 6.905 eV deviates by 4.053 eV from the value for top-level ionization, despite the fact that the difference in the corresponding single-particle energies is merely 2.341 eV. This is a clear indication that the bound-state level now splits off the band bottom and that H starts recovering its identity.

For  $N = 8$  I could not find a stable configuration with H embedded which obeys the *Aufbau* principle.<sup>38,39</sup> Whereas without H the eight electrons are accommodated in the  $1s$  and  $1p$  shells, the additional electron "does not know" where to go: With  $1s$  and  $2s$  completely filled, the fractionally filled  $1p$  level is below the  $2s$  level and with  $1s$  and  $1p$  completely filled, the fractionally filled  $2s$  level is now below the  $1p$  level. This well-known problem was encountered in our own studies on coated particles,<sup>35</sup> and for a thorough discussion of this phenomenon the interested reader is referred to the work by J. Harris.<sup>40</sup> Because we could not find a stable configuration a discussion of the energetics would not be meaningful. Hence, we turn now to a discussion of the embedding properties of He.

TABLE III. Ionization potentials (in eV) for ionization from the top level ( $I_{3p}$ ), from the bottom of the band ( $I_{2s}$ ) and (for He) from the deeply bound state ( $I_{1s}$ ). The values are compared with the energy differences of the respective single-particle levels. As a reference, the ionization potential of the "bare cluster,"  $I_0$ , is given in each case.

$N$	Bare cluster				H		He		
	$I_0$	$I_{1s}$	$I_{2s}$	$e_{12}$	$I_{3p}$	$I_{2s}$	$I_{1s}$	$e_{12}$	$e_{13}$
138	2.829	2.846	4.530	1.752	2.859	4.376	23.673	1.517	14.148
58	3.140	3.170	4.807	1.670	3.138	4.466	24.057	1.307	14.262
20	3.117	2.852	6.905	2.341	2.947	4.466	24.106	1.473	14.303
8	3.770				3.801	4.378	24.076	0.533	13.553

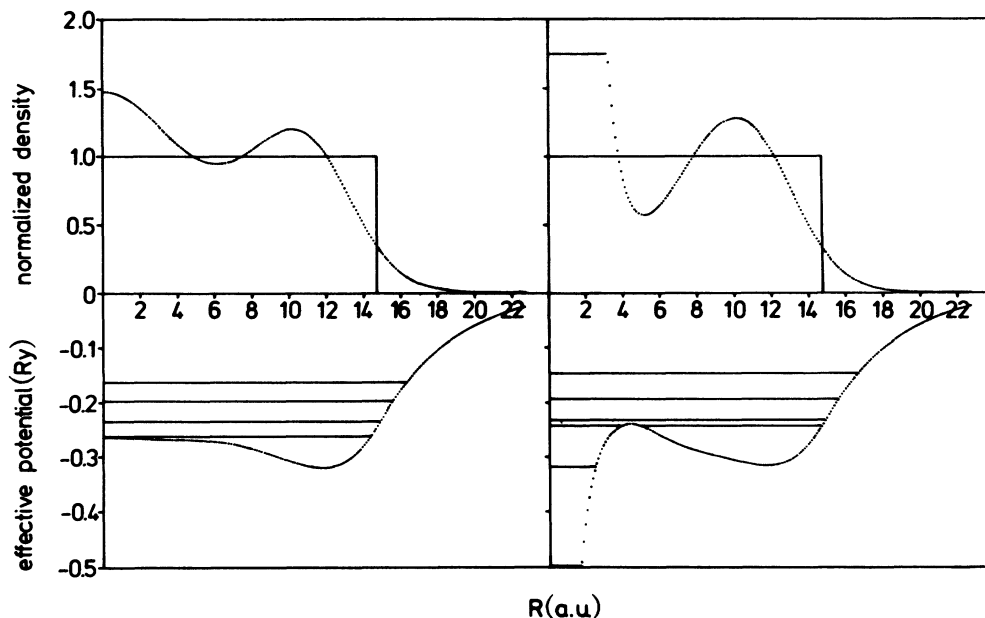


FIG. 3. The same as Fig. 1, but for  $N = 20$ . The lowest level (the  $1s$  derived from an atomic H) starts splitting off the band.

## 2. Helium

The interaction of helium with jellium, bulk or surface, is one of the best studied systems. Whereas the behavior of He in metals is of some technological importance (due to its relevance for reactor materials), the interaction of He with a metal surface is of interest because He scattering is a unique probe for testing the local electronic density at a metal surface. In this respect, the investigation of the interaction of He with small metal particles is just a continuation of these general studies with the emphasis laid on size effects. Furthermore, because of the size-dependent charge fluctuations at the center of the sphere, our results can be used as a test for the uniform density approximation (UDA) (or quasi atom approximation) due to Stott and Zaremba.<sup>41</sup>

On the other hand, He in comparison with H can serve as the simplest example to study the interaction of a strongly localized electronic level with an extended system of finite size. A problem like this is of some interest in connection with size-dependent core-level shifts,<sup>42,43</sup> and the size dependence of the core-level line shape.<sup>43</sup> Furthermore, in comparison with hydrogen, we shall see to what extent the He atom preserves its identity.

To begin with, we show in Fig. 4 self-consistently obtained charge density and potential for  $N = 138$ . The symmetry of the filled levels is, in this order,  $1s, 2s, 1p, 1d, 3s, 1f, 2p, 1g, 2d, 1h, 4s, 1i, 2f, 3p$ . As before, the  $s$  levels are pulled down dramatically, which is a first indication for the incomplete inertness of the embedded He. However, there is no visible overscreening (on the scale of this figure) which is so typical for H and other atomic systems.<sup>22</sup> Because He is the smallest closed electronic shell system in nature, its embedding features are still more localized than in the case for H. Hence, it is not surprising that its immersion energy of 0.339 eV can already be inferred from the known curve for the infinite

jellium.

The density bump at the center of the sphere (look at Fig. 1, left panel) corresponds to  $0.75n_0 = 0.0011$  a.u. For this value of the density the general curve for the immersion energy of He as a function of  $n_0$  (Refs. 23 and 44) gives 0.35 eV. Hence, we see how well the UDA of Ref. 41 works.

The next quantity of interest is the location of the  $1s$  bound level with respect to the bottom of the potential. As before we take as a measure for this the energetic difference between the truly bound level and the first band state. The result, shown in Table II, is 0.930 Ry,

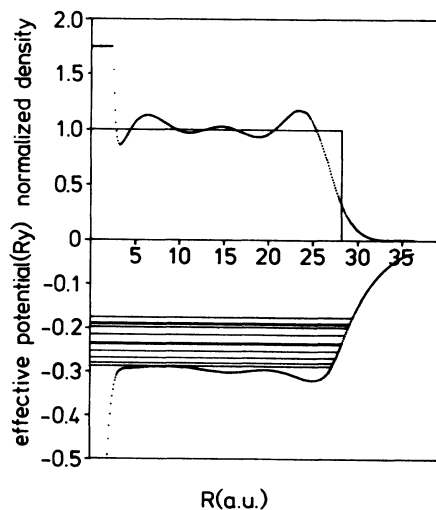


FIG. 4. The same as Fig. 1, but for He. The deeply bound  $1s$  state of the embedded He at  $-1.217$  Ry is not shown. On comparing this figure with the corresponding results of Fig. 1 it is immediately clear that He is—to a certain extent—inert. For further discussion see the text.

which compares very well with an extrapolated value of 0.94 Ry (Ref. 45) for  $r_s = 5.448$ . We turn now to the discussion of the various ionization potentials. For reasons discussed above, the following three cases were studied: Ionization from the top level of the band, ionization from the bottom level of the band, and finally ionization from the deeply bound  $1s$  state at  $-1.2154$  Ry, which is not shown in Fig. 4 (because it is so deep). The results are compiled in Table III. As was the case with H, there is no big difference in the cluster ionization potentials from the top level, with and without He, and the reason is obviously the same as before. The difference in the ionization potentials from the top level and from the band-bottom level nearly agrees with the single-particle energy eigenvalues. This tells us that the character of the states as band states does not change very much in the presence of the embedded He. Finally, the energy for ionization from the deeply bound state at  $-1.2154$  Ry is 23.673 eV, and, therefore, nearly agrees with the known value in vacuum, which is 1.7202 Ry = 23.412 eV. This value holds for our model, that is, the LDA with a Gunnarsson-Lundqvist description of the exchange-correlation functional. The nearly unchanged ionization potential is probably the strongest argument for saying that He is "inert." The fact that this value is changing only very little from 23.412 to 23.673 eV tells us that there is nearly a cancellation between initial-state effects and final-state relaxation shifts. The ionization starts from  $-1.2154$  Ry compared to  $-1.1649$  Ry in vacuum (again, of course, within the model) which means an initial-state effect of 0.687 eV towards larger binding energies. But the total energy difference is merely 0.261 eV. Hence there is some extra-atomic relaxation present which partly counterbalances the initial state shift. But, all in all, the difference is not very large and we see that it is approximately correct to speak of an embedded He as being inert. But one should not forget that there is a charge reorganization which manifests itself in the changing level scheme, concerning the  $s$  levels. From this point of view the He is not inert and resembles a little a negative ion formation, which is consistent with Zaremba's findings for the infinite jellium.<sup>41,44</sup>

The results for the other particle numbers are very similar, so we give only a short account of these data. From Table I we learn that the immersion energy follows closely the infinite jellium result, taken at the density bump or hump, respectively, at the center of the sphere. Especially the value of 0.691 eV for  $N=20$  is in perfect agreement with the value we would obtain for the density at  $r=0$ , namely 0.69 eV for  $n_0=0.0022$  a.u. (see Fig. 5). So we see that the embedded He is indeed nearly ideally localized. It is not before  $N=8$  that this simple picture starts changing towards the vacuum behavior. The binding energy of the  $1s$  state relative to the bottom of the band, shown in Table II, behaves very similarly. Small fluctuations are a combination of changes due to variations in the local density around the impurity and due to quantum size effects in the band-bottom level. Again at  $N=8$ , the level starts moving towards the vacuum level of the model, namely to  $-1.1649$  Ry. The various ionization potentials, shown in Table III, corroborate the

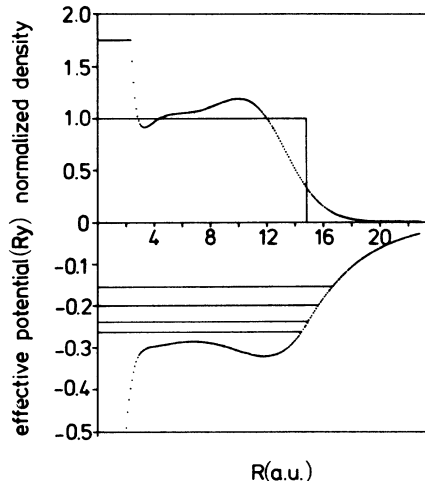


FIG. 5. The same as Fig. 4, but for  $N=20$ .

conclusions drawn from the immersion energy and from the binding of the bound state. The ionization from the  $1s$  level fluctuates a little and will certainly converge towards the vacuum level at  $-1.7202$  Ry.

To conclude this section, let us repeat the most important finding about the He embedding: The embedded He is a highly inert system as far as the behavior of the He itself is concerned. However, from the change of the  $s$  levels of the particle upon He embedding we conclude that the host density  $\rho$  is being disturbed. This does not mean necessarily that a big change in the total density is to be expected. What is changing is the local density of states.

### III. SIZE-DEPENDENT POLARIZABILITY

The size dependence of the polarizability plays traditionally a major role when discussing size effects (or quantum-size effects) in the physics of small metal particles. One of the reasons is certainly the importance small particles have as scattering centers for electromagnetic waves in astrophysics. This might explain that the classical theory of light scattering by small particles is well known for nearly one century.<sup>46</sup> On the other hand, size effects are of general physical interest and have been studied for a number of years by both experimentalists and theoreticians. Hence, a large quantity of literature exists and the interested reader is referred to the recent review by Halperin.<sup>47</sup>

For practical reasons, the matrix isolation technique is widely used when investigating small metal particles. This makes a direct comparison between theory and experiment impossible. However, the situation is more favorable in the case of the alkali-metal clusters, for which Knight *et al.* were able to measure, over a wide range of particle numbers, both the static polarizability and the ionization potential and efficiency.

Measurements on the plasma resonance will be done very soon<sup>48</sup> and experiments on H embedding are in preparation.<sup>49</sup> Hence, I believe that there is both a practical and a general theoretical interest for studying the

dynamical properties of jellium clusters in the presence of impurities.

### A. Method of calculation

The method of calculation is the so-called time-dependent local-density approximation (TDLDA) which has been successfully applied to the photoabsorption and photoemission from atoms, molecules, solid surfaces, and clusters. The method was independently proposed in 1980 by Zangwill and Soven,<sup>50</sup> by Stott and Zaremba,<sup>51</sup> and in a slightly different form by Mahan.<sup>52</sup> Because the method is now widely in use we do not give any detailed explanation but refer the interested reader to the original work and to our own work concerning the application of the TDLDA to small jellium clusters<sup>53</sup> (see also Puska *et al.*<sup>54</sup> and Beck<sup>55</sup>).

#### 1. Static polarizability

The static polarizability of an ideal metal sphere is known to be given by the cube of its radius,  $R^3$ . Hence it is common, when discussing size effects on the static polarizability of small particles, to discuss the ratio of the actual polarizability and the classical one. Whereas non-self-consistent calculations of this ratio give typically a value smaller than one which, furthermore, is strongly size dependent,<sup>56</sup> the self-consistently obtained results show only a weak size dependence and the value is larger than 1.<sup>53–55</sup> This result is more or less experimentally confirmed by measurements of Knight *et al.*<sup>12</sup> for Na, which corresponds to a  $r_s$  value of 4. Specific measurements for an  $r_s$  value of 5.4481 have not been done yet but are planned for the near future.<sup>57</sup> (Remember, this  $r_s$  is near to the  $r_s$  value of Cs).

The main question in the present study is as follows: Are there any typical impurity-induced size effects on the static polarizability compared to the one of the cluster without impurity? The answer to this question, as far as the static case is concerned, is given in Table IV (and follows already from the discussion in Sec. II). Because of the strong localization of the impurity, and because of the fact that the polarization charge in the presence of a static electric field is strongly localized on the surface of the particle, only a marginal change is to be expected for this quantity. Indeed, on looking at Table IV we see that there is virtually no change from the bare cluster polarizability. The value of 1.961 for H embedding at  $N=8$  is a little misleading because it is this structure where we could not find an “Aufbau-principle” ground state. For

TABLE IV. Size dependence of the static polarizability of the jellium clusters with H and He embedded. For comparison, the “bare cluster” value is given in the third column. All values are in units of the classical value, namely  $R^3$ .

$N$	$R$	Bare cluster	H	He
138	28.154	1.111	1.112	1.109
58	21.089	1.167	1.137	1.134
20	14.788	1.218	1.177	1.260
8	10.986	1.263	1.961	1.217

all other cases, it would be very hard and virtually impossible to see any effect of the impurity. Hence, we turn to the discussion of the dynamical effects where measurable effects *are* to be expected.

#### 2. Dynamical polarizability

From the dynamical polarizability of a system we get information about the excitation spectrum. As explained at length in our previous work<sup>53,55,57</sup> the dominant feature of the dynamical polarizability of a small jellium cluster is the size-dependent analogue of the classical Mie resonance of a particle, namely, in more modern language, the dipolar surface plasmon of a metallic sphere (to be exact, the nonretarded version of the Mie resonance). In addition, and in sharp contrast to the classical theory, the spectrum comprises single particle-hole pairs and, even in the optical excitation mode, charge density oscillations of the volume type. The size dependencies of these quantities are now well understood and, as remarked above, the first experimental results taken on the cluster beam in the gas phase should appear very soon.

The questions to answer in the present case are as follows:

- (1) What is the effect of the impurity on the intrinsic excitation spectrum of the cluster?
- (2) How are the impurity transitions modified upon immersion in the cluster?
- (3) Are there any characteristic differences between an inert system like He and a reactive one like H?

The answer to all these questions is implicitly contained in the figures to follow.

Figure 6 gives, on a logarithmic scale, the imaginary part of the dynamical polarizability, in units of  $R^3$ , of (a) the bare cluster, (b) the cluster with H embedded, and (c) the cluster with He embedded. The polarizability is given on a logarithmic scale and the particle number is  $N=138$ . The frequency  $\omega$  is given in units of the frequency of the classical surface plasmon frequency of the particle, which is  $\omega_p/\sqrt{3}$ , with  $\omega_p$  the plasma frequency  $4\pi n_0 e^2/m$ , where  $n_0$  is the electronic density and  $m$  the mass of the electron. For comparison the figures contain two more curves: The dashed one gives the independent electron result, and the dotted one gives the classical result. From a comparison of all these curves we learn (1) something about the formation of collective modes at the cost of single pair motion, and (2) something about the size-induced quantum effects. The general discussion was performed in our previous work<sup>35,53,57</sup> and will not be repeated here. For numerical details in performing the calculations the interested reader is referred especially to Ref. 53.

The figures reveal at least two remarkable results, namely (1) there is virtually no difference between the bare cluster and the cluster with He embedded (in the frequency range shown in the figure), and (2) there are changes in the bare cluster polarizability upon which H was embedded. These can clearly be identified as (a) an enhanced red shift and an additional broadening of the

dipolar surface plasmon around 0.9 and, more pronounced, (b) the approximate quenching of the various dipolar volume plasmons at the frequencies 1.79, 1.97, and 2.28.

We think that all these results are understandable from the previous discussions. The nearly unchanged polarizability upon He embedding is just one more example of its inertness (for higher frequencies, see the discussion below).

The H results are a consequence of the impurity-induced enhanced inhomogeneity of the electronic charge density which leads, in turn, to an enhanced Landau damping of collective motion. That the effect is more pronounced for the volume modes is easy to understand because the charge density for the surface plasmon is mainly sensitive to changes in the surface region. Hence, the additional broadening of the surface plasmon is just

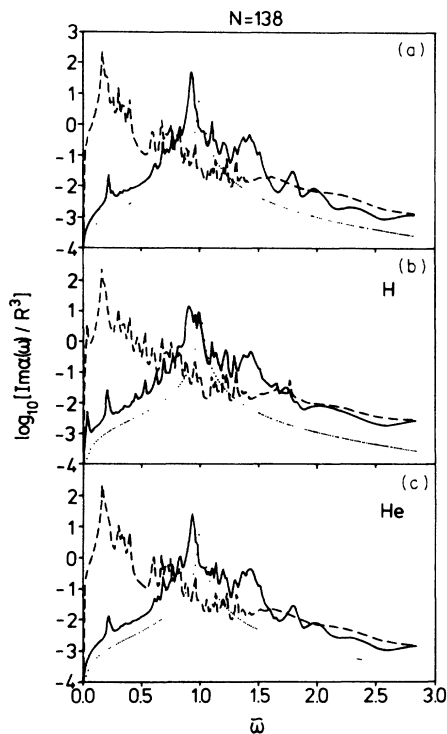


FIG. 6. Frequency dependence of the imaginary part of the dynamical polarizability of the jellium clusters of Figs. 1 and 4: (a) bare cluster, (b) with H embedded, and (c) with He embedded. The polarizability is, on a logarithmic scale, in units of  $R^3$  and the frequency is in units of the classical dipolar surface plasmon frequency of a sphere. The actual polarizability (solid line) is compared with the classical one (dots) and with the independent electron result (dashed line). As discussed in the text, the actual polarizability is calculated within the TDLDA. In this context, the dashed line is nothing other than the LDA polarizability. The actual polarizability is governed by the red-shifted Mie resonance at  $\tilde{\omega} \approx 0.9$ , by numerous particle-hole pairs, and by a number of size-quantized, blue-shifted dipolar volume plasmons (above the classical value at 1.723 in the units used in the figure). The quenching of the collective volume modes upon H embedding can clearly be seen. In addition, the surface plasmon of the bare cluster is even more red-shifted and gets additional broadening. For further discussion see the text.

an impurity-induced volume contribution to the total rate of damping, whereas for the volume mode it seems to be more important that all the  $s$  states undergo a major change in their charge densities around the center of the sphere. Additional impurity-induced single-pair transitions are well resolved in the case of H, but would be hardly detected because of their small oscillator strength (but see the discussion below for He).

After this very detailed explanation for  $N = 138$  we give only a very short discussion for the other particle numbers, namely  $N = 58$  (Fig. 7) and  $N = 20$  (Fig. 8). The results for  $N = 58$  are nearly the same as they were for  $N = 138$ , hence we turn immediately to  $N = 20$ . On looking at Fig. 8 we see that at this low particle number a pronounced change occurs not only upon H embedding but also upon He embedding. The reason for this change mainly in the particle-hole part of the spectrum is the different shell for accommodating the screening charge. Whereas for H the  $1f$  level is singly occupied and the  $3s$  level is completely empty the latter level is pulled down upon He immersion and now accommodates two electrons. So in the case of H we have a relatively open structure with one loosely bound electron in the  $1f$  shell, whereas in the case of He we have a relatively compact structure with 3  $s$  shells completely occupied. All this leads to major changes, especially in the single-pair features in the spectral range covered in the figure. The result is in complete agreement with general trends about the importance of individual particle-hole pairs at smaller particle numbers, found in our previous studies.

Finally, in the Fig. 9, we turn to the discussion of transitions from the deeply bound  $1s$  state of He to the size-quantized empty states in the conduction band. The ad-

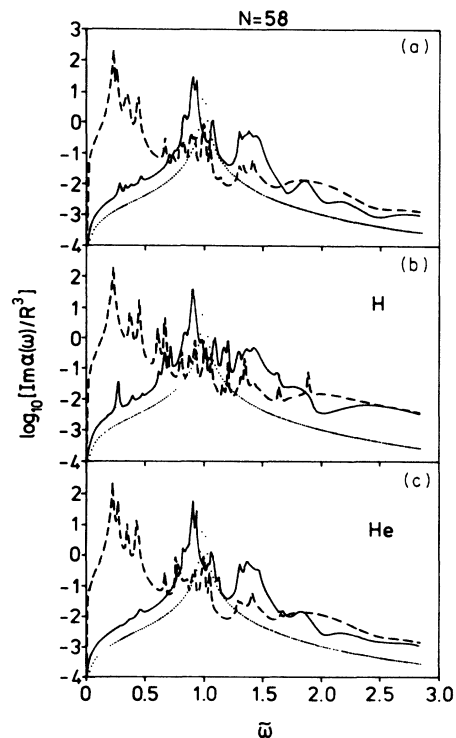


FIG. 7. The same as Fig. 6, but for  $N = 58$ . There is no big change compared to the results for  $N = 138$ .



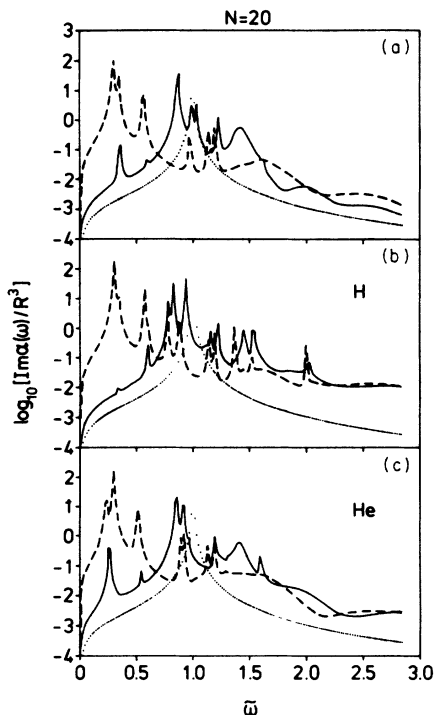


FIG. 8. The same as Fig. 6, but for  $N = 20$ . Now, we observe major changes in the polarizability which are discussed in full detail in the text.

vantage of a spectroscopic investigation of these transitions is obvious: There are no other transitions around and, especially, no collective modes which can dominate the spectral region. From these figures we learn that probably the best way of verifying the size quantization in the conduction band would be the excitation of deep core states of a metal like Na to the size-quantized conduction levels. All the transitions are well separated because of the existence of optical selection rules (like  $s$ - $p$ , etc). Surprisingly enough the transitions under discussion are not monotonic but rather oscillating. This is caused both by fluctuations in the initial state and in the empty final states and is, again, related to the changing configuration of occupied levels as discussed above.

#### IV. CONCLUSION

In this work we have investigated static and dynamical properties of H and He embedded in small jellium clusters as an example for the interaction of reactive and inert localized systems with small metal particles. The expectation that He as a closed shell system is "inert" is approximately correct both for the He properties itself and for its influence on the various properties of the jellium cluster. We have found that, due to its localized nature, the immersion energy follows the trends predicted by the UDA. The ionization potential is slightly enhanced and the relative binding energy of the deeply bound  $1s$  state with respect to the lowest band state is very similar to the value known for the infinite system. Perturbations of the various cluster properties are always very small except for some changes in the  $s$  components of the charge den-

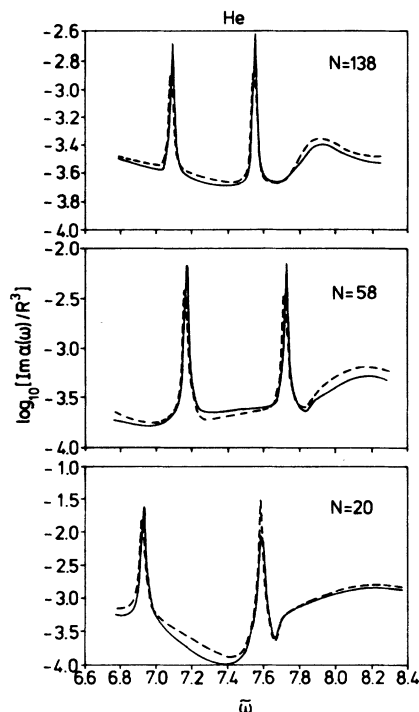


FIG. 9. The size dependence of the transitions from the deeply bound  $1s$  level of He to the size-quantized empty  $p$  levels in the conduction band. As argued in the text, this would be an ideal test case for a direct verification of the size quantization in general. The transition frequencies are fluctuating for reasons discussed at the end of Sec. III.

sity around the He. The influence on the dynamical properties is very small except for some particle-hole-pair transitions at very small electron numbers ( $N < 20$ ).

The situation is completely different for H. Because it is an open-shell system it has a major influence on the various cluster properties and, vice versa, its "own" properties undergo a strong modification upon immersion in a jellium cluster. Probably the most interesting finding is the role H plays for the quenching of collective motion. After all, this is to be expected, as the embedding of H causes a strong charge disturbance in the host. For this reason the effect is more pronounced for the volume modes than it is for the surface mode because the latter effect is oscillating mainly on the surface of the particle.

Finally, we want to come back to a discussion of the magic numbers. As we have seen in the various examples, there is a reordering of the  $s$  levels of the host particle in both cases, for H and for He. As a consequence, the magic numbers are expected to change upon impurity embedding. Even more, because the  $s$  levels are more strongly bound in the presence of an impurity we expect a more pronounced structure in the abundance spectra whenever an  $s$ -level shell becomes completely filled. The effect will be similar if H is not at the center of the sphere but anywhere else in the volume. Because H embedding is a more or less localized process, one electron will be accommodated in the deepest ( $1s$ ) shell and, as a result, this quantity is a weak perturbation on the rest of the system. Hence, one electron disappears from the system of loose-

ly bound valence electrons. The situation resembles that of the problem of cluster growth, born neutral or born ionized. Because of the doubly occupied "deep" 1s shell the magic numbers should change to those of a "positively born" particle. To be specific, in a system of  $N$  Na atoms and one H atom the magic mass numbers concerning the Na change from  $N$  to  $N + 1$ . The generalization of this idea to more than one H is obvious.

The situation for He is not as obvious as in the case of H. But still, we have the general rules discussed above.

#### ACKNOWLEDGMENTS

The author is grateful to Professor E. Zeitler for continuing interest and support. Many thanks are due to R. Fuchs for critically reading the manuscript and for constructive remarks.

- <sup>1</sup>J. L. Martins, R. Car, and J. Buttet, *Surf. Sci.* **106**, 265 (1981).  
<sup>2</sup>W. Ekardt, *Phys. Rev. B* **29**, 1558 (1984).  
<sup>3</sup>D. E. Beck, *Solid State Commun.* **49**, 381 (1984).  
<sup>4</sup>A. Hintermann and M. Manninen, *Phys. Rev. B* **27**, 7262 (1983).  
<sup>5</sup>M. Y. Chou and Marvin L. Cohen, *Phys. Lett.* **113A**, 420 (1986).  
<sup>6</sup>W. D. Knight, K. Clemenger, W. A. de Heer, W. Saunders, M. Y. Chou, and Marvin L. Cohen, *Phys. Rev. Lett.* **52**, 2141 (1984).  
<sup>7</sup>W. D. Knight, W. A. de Heer, K. Clemenger, and W. Saunders, *Solid State Commun.* **53**, 445 (1985).  
<sup>8</sup>W. D. Knight, W. A. de Heer, W. Saunders, K. Clemenger, M. Y. Chou, and Marvin L. Cohen, *Chem. Phys. Lett.* **134**, 1 (1987).  
<sup>9</sup>I. Katakuse, T. Ichihara, Y. Fujita, T. Matsuo, T. Sakurai, and H. Matsuda, *Int. J. Mass. Spec. Ion Proc.* **67**, 229 (1985).  
<sup>10</sup>I. Katakuse, T. Ichihara, Y. Fujita, T. Matsuo, T. Sakurai, and H. Matsuda, *Int. J. Mass. Spec. Ion Proc.* **69**, 109 (1986).  
<sup>11</sup>I. Katakuse, T. Ichihara, Y. Fujita, T. Matsuo, T. Sakurai, and H. Matsuda, *Int. J. Mass. Spec. Ion Proc.* **74**, 33 (1987).  
<sup>12</sup>W. D. Knight, K. Clemenger, W. A. de Heer, and W. Saunders, *Phys. Rev. B* **31**, 2539 (1985).  
<sup>13</sup>W. Saunders, K. Clemenger, W. A. de Heer, and W. D. Knight, *Phys. Rev. B* **32**, 1366 (1985).  
<sup>14</sup>K. Clemenger, *Phys. Rev. B* **32**, 1359 (1985).  
<sup>15</sup>Z. D. Popovic and M. J. Stott, *Phys. Rev. Lett.* **33**, 1164 (1974).  
<sup>16</sup>M. D. Whitmore, *J. Phys. F* **6**, 1259 (1976).  
<sup>17</sup>R. Benedek, *J. Phys. F* **8**, 807 (1978).  
<sup>18</sup>C. O. Almbladh, U. von Barth, Z. D. Popovic, and M. J. Stott, *Phys. Rev. B* **14**, 2250 (1976).  
<sup>19</sup>E. Zaremba, L. M. Sander, H. B. Shore, and J. H. Rose, *J. Phys. F* **9**, 1763 (1977).  
<sup>20</sup>P. Jena and K. S. Singwi, *Phys. Rev. B* **17**, 3518 (1978).  
<sup>21</sup>M. Manninen, P. Hautojärvi, and R. Nieminen, *Solid State Commun.* **23**, 795 (1977).  
<sup>22</sup>G. W. Bryant and G. D. Mahan, *Phys. Rev. B* **17**, 1744 (1978).  
<sup>23</sup>M. J. Puska, R. M. Nieminen, and M. Manninen, *Phys. Rev. B* **24**, 3037 (1981).  
<sup>24</sup>G. D. Mahan, *Phys. Rev.* **163**, 612 (1967).  
<sup>25</sup>P. Nozières and C. T. de Dominicis, *Phys. Rev.* **178**, 1097 (1969).  
<sup>26</sup>O. Gunnarsson B. I. Lundqvist, *Phys. Rev. B* **13**, 4274 (1976).  
<sup>27</sup>I. I. Geguzin, *Phys. Tverd. Tela (Leningrad)* **24**, 439 (1982) [*Sov. Phys.—Solid State* **24**, 248 (1982)].  
<sup>28</sup>A. N. Cleland and Marvin L. Cohen, *Solid State Commun.* **55**, 35 (1985).  
<sup>29</sup>B. K. Rao, P. Jena, M. Manninen, and R. M. Nieminen, *Phys. Rev. Lett.* **58**, 1188 (1987).  
<sup>30</sup>Jose Luis Martins, Jean Buttet, and Roberto Car, *Phys. Rev. B* **31**, 1804 (1985).  
<sup>31</sup>F. R. Redfern, R. C. Chaney, and P. G. Rudolf, *Phys. Rev. B* **32**, 5023 (1985).  
<sup>32</sup>We propose to call this model the Sommerfeld droplet model because it is a combination of the liquid drop model of nuclear physics and the Sommerfeld model for  $sp$  metals. As we shall see from Ref. 33, the shape of the particle changes like that of an incompressible liquid and, at the same time, the bottom of the potential relative to the vacuum zero stays nearly constant.  
<sup>33</sup>W. Ekardt and Z. Penzar (unpublished).  
<sup>34</sup>This special  $r_s$  value, which is approximately that of Cs ( $= 5.62$  a.u.) results from a comparative study (to follow) with coated particles and "jellium alloys," where we needed special particle numbers and shell structures to fulfill the *Aufbau* principle for mixtures of  $r_s = 4$  and 6. To save computer time we had to make a compromise concerning special combinations of  $r_s$  values and total particle numbers.  
<sup>35</sup>W. Ekardt, *Phys. Rev. B* **34**, 526 (1986).  
<sup>36</sup>P. Jena and K. S. Singwi (Ref. 20) give for  $r_s = 5$  the value of 0.016 Ry.  
<sup>37</sup>J. F. Janak, *Phys. Rev. B* **18**, 7165 (1978).  
<sup>38</sup>L. Hedin and S. Lundqvist, *Solid State Phys.* **23**, 1 (1969).  
<sup>39</sup>J. P. Perdew and A. Zunger, *Phys. Rev. B* **28**, 5048 (1981).  
<sup>40</sup>J. Harris, *Phys. Rev. A* **29**, 1648 (1984).  
<sup>41</sup>M. J. Stott and E. Zaremba, *Phys. Rev. B* **22**, 1564 (1980).  
<sup>42</sup>G. Apai, J. F. Hamilton, J. Stöhr, and A. Thompson, *Phys. Rev. Lett.* **43**, 165 (1979).  
<sup>43</sup>T. P. Cheung, *Surf. Sci.* **140**, 151 (1984).  
<sup>44</sup>M. J. Stott and E. Zaremba, *Solid State Commun.* **32**, 1297 (1979).  
<sup>45</sup>I am grateful to Eugene Zaremba for providing these data for  $r_s$  values of 1.6, 2, 3, 4, 5. For larger  $r_s$  values no data exist because of problems with the convergence in infinite jellium systems.  
<sup>46</sup>G. Mie, *Ann. Phys. (Leipzig)* **25**, 377 (1908).  
<sup>47</sup>W. P. Halperin, *Rev. Mod. Phys.* **58**, 533 (1986).  
<sup>48</sup>W. A. de Heer, K. Selby, V. Kresin, J. Masui, A. Chatelain, and W. D. Knight, *Bull. Am. Phys. Soc.* (1987).  
<sup>49</sup>W. A. de Heer (private communication).  
<sup>50</sup>A. Zangwill and P. Soven, *Phys. Rev. A* **21**, 1561 (1980).  
<sup>51</sup>M. J. Stott and E. Zaremba, *Phys. Rev. A* **21**, 12 (1980).  
<sup>52</sup>G. D. Mahan, *Phys. Rev. A* **22**, 1786 (1980).  
<sup>53</sup>W. Ekardt, *Phys. Rev. B* **31**, 6360 (1985).  
<sup>54</sup>M. J. Puska, R. M. Nieminen, and M. Manninen, *Phys. Rev. B* **31**, 3486 (1985).  
<sup>55</sup>D. E. Beck, *Phys. Rev. B* **30**, 6935 (1984).  
<sup>56</sup>M. J. Rice, W. R. Schneider, and S. Strässler, *Phys. Rev. B* **8**, 474 (1973).  
<sup>57</sup>W. Ekardt, *Phys. Rev. Lett.* **52**, 1925 (1984).